Exploration of Medicine

Open Exploration

Open Access Original Article

Pyogenic liver abscess: contrast-enhanced ultrasound allows morpho-evolutive classification and guides personalized management

Giampiero Francica*

Interventional Ultrasound Unit, Pineta Grande Hospital, 81030 Castel Volturno (CE), Italy

*Correspondence: Giampiero Francica, Interventional Ultrasound Unit, Pineta Grande Hospital, Via Domitiana km 30,00, 81030 Castel Volturno (CE), Italy. giampierofrancica@gmail.com

Academic Editor: Lindsay A. Farrer, Boston University School of Medicine, USA

Received: April 5, 2022 Accepted: May 18, 2022 Published: June 28, 2022

Cite this article: Francica G. Pyogenic liver abscess: contrast-enhanced ultrasound allows morpho-evolutive classification and guides personalized management. Explor Med. 2022;3:289–99. https://doi.org/10.37349/emed.2022.00093

Abstract

Aim: The aim of this study is to propose a contrast-enhanced ultrasound (CEUS)-based morphologic classification of pyogenic liver abscess (PLA) reflecting different evolutive stages and to assess the added value of CEUS in the management of PLA.

Methods: Forty-four PLAs of different etiologies in 44 patients (male/female = 24/20; mean age 66 ± 14.7 years) were evaluated with ultrasound (US) B-mode and CEUS (using SonoVue). PLAs were mainly located in the right lobe (*n* = 28, 63.6%) with a mean diameter of 6.8 cm [standard deviation (SD) ± 3.2, range 1.7–15 cm]. Conventional US findings were categorized as the presence and extension of liquified areas, echogenicity and echostructure of the index lesion. Peripheral hyperenhancing rim, transient segmental enhancement, hyperenhancing septa and "honeycomb" aspect were considered PLA hallmarks in the arterial phase after contrast agent injection. CEUS results were judged as clinically relevant if they modified the approach to percutaneous treatment in comparison with pre-operative US B-mode findings.

Results: CEUS was superior to US B-mode as to depiction of PLA internal echostructure and enabled identification of 4 evolutive stages of PLA: type I (tumor-like), type II ("honeycomb"), type III (multiloculated with incomplete septa), and type IV (cystic-like). In 22 cases (67.4%) out of 34 who underwent percutaneous treatment, the operator tailored percutaneous approach according to PLA internal echostructure observed during CEUS exam.

Conclusions: CEUS depicts the internal structure of PLA so allowing a morpho-evolutive classification of PLA and provides invaluable information for immediately tailoring the management to the single case. By showing the structure of PLA more precisely, CEUS allows a morpho-evolutive PLA classification and guides tailored management in the single case.

Keywords

Contrast-enhanced ultrasound, abscess, liver, drainage

Introduction

Hepatic abscess is defined as a suppurated cavity caused by the invasion and multiplication of microorganisms within healthy or diseased liver parenchyma, and it may be caused by bacteria, fungi, and parasites [1]. When the causative agents are bacteria, hepatic abscess is called pyogenic liver abscess (PLA) [2, 3].

The incidence rate of PLA in the western countries has been estimated to range between 3.59 and 2.9 per 100,000 population years based on different population-based studies [4, 5]. In Western countries, 80% of PLA are bacterial, mainly *Escherichia coli* (*E. Coli*) and *Streptococcus* spp. [6], but recent reports reveal that incidence of *Klebsiella pneumoniae* in the Western hemisphere is increasing [7]. The most common presenting clinical symptoms, right upper quadrant pain, fever, rigors, and jaundice vary from mild to severe. Clinically occult abscess may simply present with malaise, weight loss and vague abdominal pain [2, 5].

PLA can occur in the course of intra-abdominal biliary infections that contaminate the biliary tract at the same time or can be secondary to seeding via the portal venous system of non-biliary infections (appendicitis or diverticulitis) [8, 9]. It has been suggested that PLA might be an indicator of gastrointestinal cancer, particularly occult colon cancer [10]. PLA can also complicate surgical procedures (pancreatoduodenectomy, or liver transplantation) or hepatobiliary procedures (thermal ablation and/or intra-arterial chemoembolization). More rarely, PLA develops after liver trauma or arterial embolization for trauma [8, 9]. Nevertheless, it is estimated that up to 40% of liver abscesses have no recognizable route to the liver and are labeled cryptogenic [9].

Diagnostic imaging has a vital role in suspected cases of liver abscess. Contrast-enhanced computed tomography (CECT) and ultrasound (US) are the primary tools used to image the liver. The US and CECT sensitivities for diagnosis of PLA are 85% and 97%, respectively [11, 12]. At US, microabscesses (< 2 cm) appear as hypoechoic nodules or ill-defined areas of distorted hepatic echogenicity [13]. Large abscesses range from hypoechoic to hyperechoic masses, depending on the presence of internal echoes due to thickened septa and debris [13, 14]. More recently, the introduction of US contrast agent has improved characterization of focal liver lesions [15] and contrast-enhanced ultrasound (CEUS) features of PLA have been described [15, 16]. The most typical CEUS findings, i.e., the non-enhancement of the liquefied portions combined with arterial rim enhancement, refer to the mature stage of PLA, but additional findings such as presence of hyperenhanced septa and transient segmental enhancement (TSE) at the periphery of PLA in the arterial phase have been reported [15–17]. CEUS has been shown to improve PLA diagnosis in comparison with US B-mode [18], achieving the same diagnostic accuracy rates as CECT and magnetic resonance imaging (MRI) [19].

In combination with targeted antimicrobial therapy, percutaneous drainage techniques [through catheter positioning and/or needle aspiration (NA)] are considered the mainstay of treatment for PLA [1, 20, 21], whereas surgery (simple drainage or even hepatectomy) may be done if other forms of treatment have failed or in special circumstances when PLAs are multiple or very large and multiloculated [21–23].

The aim of this study is to propose a CEUS-based morphologic classification of PLA reflecting different evolutive stages and to assess the added value of CEUS in the management of PLA.

Materials and methods

Series

Forty-four patients with PLA were seen between January 2016 and December 2021. Demographic characteristics of the PLAs studied are shown in Table 1. In the 8 patients with multiple PLAs, only the greatest ones were considered for the study.

Table 1. Main characteristics of the PLAs studied with CEUS*

Demographic characteristics	PLAs values
No patients	44
No male/female	24/20
Mean age (years ± SD)	66 ± 14.7
No PLAs	44
Mean size (cm ± SD)	6.8 ± 3.2
Site right/left	28/16
Etiology	
Neoplasia (colon/pancreas/biliary tract)	2/4/4
Acute calculous cholecystitis	8
Choledocholithiasis	7
Intrahepatic lithiasis	3
Post-surgery	6
Idiopathic	5
Diverticulitis	2
Diabetes	2
Foreign body	1
Symptoms	
Fever > 38°C	40
Jaundice	11
Abdominal pain	35
Malaise	8

*In 8 patients with multiple PLA only the largest one was studied with CEUS. SD: standard deviation

Technique and equipment

Just after conventional US exam, all patients underwent CEUS according to the usual modality: SonoVue (sulfur hexafluoride with a phospholipid shell; Bracco SpA, Milan, Italy) was administered IV as 2.4 mL boluses through the antecubital vein in 2–3 seconds, followed by a 5 mL flush of normal saline (0.9%). US equipment used over the study period had dedicated software for contrast specific imaging (MyLab™Twice, Esaote, Genova, Italy; Resona 7 system, Mindray Bio-Medical Electronic Co., Shenzhen, People's Republic of China).

All US B-mode and CEUS images were retrospectively evaluated by a single operator (the same who carried out the initial US and CEUS examinations) with more than 20-year experience in US contrast agent examination of the liver.

US B-mode and CEUS findings

Conventional US findings were categorized as to the presence and extension of liquified areas, echogenicity and echostructure (if solid-like, cystic-like or mixed) of the index lesion.

Peripheral hyperenhancing rim (PHR), TSE, hyperenhancing septa (complete or incomplete) and "honeycomb" aspect (i.e., multiple liquified areas separated by hyperenhancing septa) were considered in the arterial phase after injection of contrast agent; enhancement behaviors of PHR, TSE and septa were assessed in portal and venous late phases as well.

Broad spectrum antibiotics were usually administrated for all patients until results of the laboratory tests were available and modified according to the causative organisms identified on blood culture and/or aspirated material.

Treatment

Thirty-four patients with PLA > 4 cm underwent US-guided percutaneous treatment by means of catheter drainage (CD) and/or NA; 2 patients had surgical resection and the remaining 8 cases received antibiotic therapy only.

All interventional procedures were carried out by a single operator (the same who performed and reviewed US and CEUS imaging) with more than 30-year experience in interventional US.

Impact on treatment

To assess clinical impact of CEUS in the interventional management of PLA, CEUS results were judged as clinically relevant if they modified one among the following therapeutic choices in comparison with pre-operative US B-mode results: 1) CD *vs.* NA; 2) combination of NA and CD; 3) use of single *vs.* multiple catheters according to the presence of communication between compartments of complex abscess cavities.

Follow-up

The patients were studied with imaging (one or more examinations among US, CEUS, CECT, and MRI) during follow-up to monitor PLA evolution.

Informed consent

This retrospective study was approved by the Pineta Grande Hospital Institutional Review Board and a signed informed consent was obtained from all patients before US contrast media contrast injection and US-guided interventional procedures.

Results

PLAs were mainly located in the right lobe (n = 28, 63.6%) with a mean diameter of 6.8 cm (SD ± 3.2, range 1.7–15 cm). As far as etiology was concerned, benign (n = 10) and malignant (n = 8) obstruction accounted for 34% of the cases whereas PLA synchronous with acute cholecystitis was found in 18% of the cases. Main presenting symptoms were fever > 38°C, abdominal pain, and jaundice.

Causative organisms were detected in 60% of the drained material and in 42% of blood culture (mostly *E. Coli*, *Streptococcus* spp., *Klebsiella Pneumoniae* and mixed).

US B-mode

Most of the lesions (16 = 36.4%) showed a complex heterogeneous echostructure due to alternating areas of hypo/hyperechogenicity and fluid levels (Figure 1a); the second most frequent US appearance (13 = 29.5%) was that of a large liquified area surrounded by a thick capsule (cystic-like) (Figure 1b). The most challenging US presentation was found in PLAs with a solid, more often hypoechoic with or without a small liquified central area, mimicking liver tumors (9 = 20.4%) (Figure 1c).

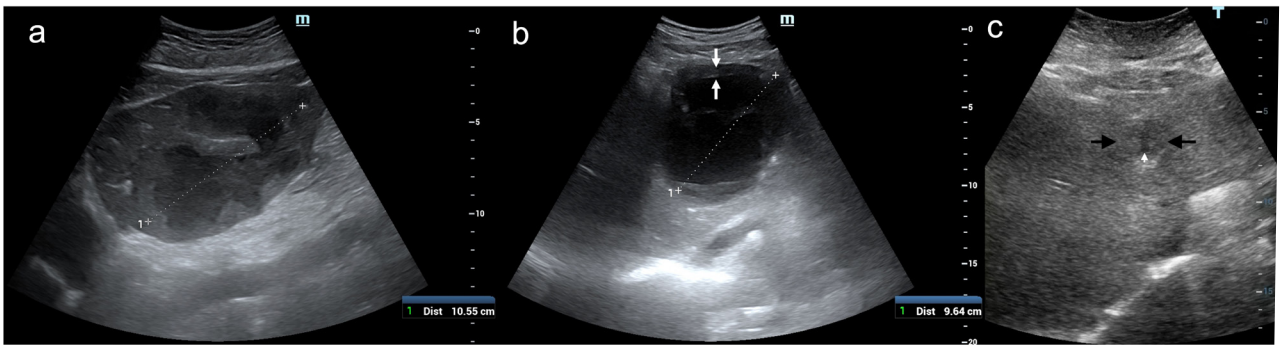

Figure 1. US B-mode patterns of PLA. (a) A large (11 cm) heterogeneous solid mass with fluid levels occupies the left liver lobe; (b) cystic-like PLA: a thick solid capsule (between white arrows) encircles a large colliquated cavity of 9.6 cm; (c) tumor-like PLA: a 4-cm poorly visible, hypoechoic lesion (between black arrows) with a small, central liquid area (black arrows)

CEUS

In the early arterial phase after contrast agent injection the most frequent findings were TSE (40 = 91%), non-enhanced (liquified) areas of different sizes and numbers (39 = 88%) and PHR of variable thickness (38 = 86.4%) (Figure 2). Presence of hyperenhancing septa of variable width and extension occurred in 24 PLAs (54.5%) during the arterial phase (Figure 2b). The so-called "honeycomb" aspect due to alternating liquified area and hyperenhanced septa was found in 12 cases (27.3%) (Figure 3).

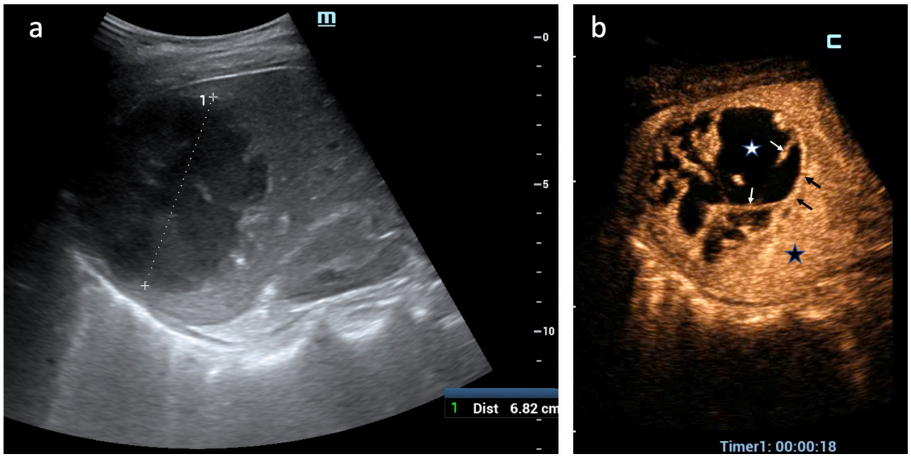

Figure 2. CEUS findings in PLA (arterial phase). (a) A 7-cm PLA is displayed in the right liver lobe at US B-mode; (b) TSE (black star) surrounds PLA; a thin PHR (black arrows) delimits abscessed cavity where irregular non-enhanced areas of liquefaction (white star) are separated by hyperenhancing septa (white arrows). Based on CEUS demonstration of communication between the multiple liquified cavities, the operator confidently positioned a single 8-F catheter to drain PLA

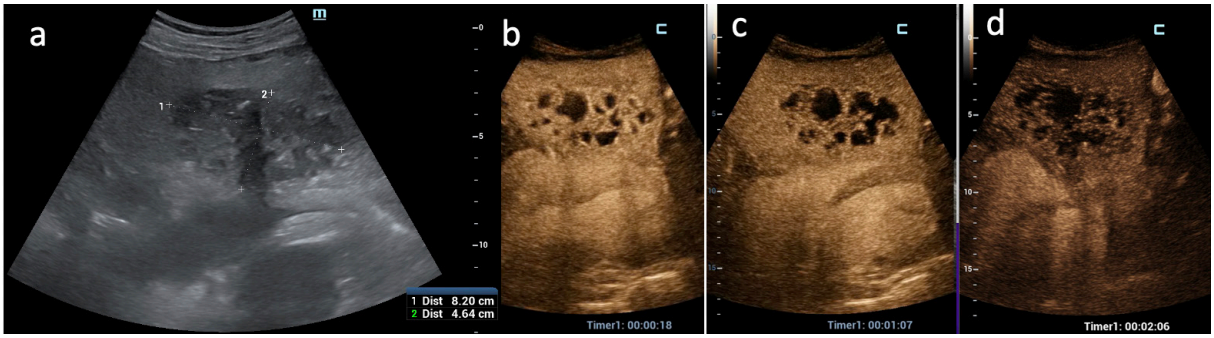

Figure 3. CEUS PLA type II. (a) An 8-cm solid mass of the left hepatic lobe is displayed at US B-mode; (b) in the arterial phase after US contrast agent injection a typical "honeycomb" pattern is displayed due to alternating small, liquified (non-enhanced) areas and inflamed (hyperenhanced) parenchyma; (c–d) in the portal and late venous phases the solid components become hyperenhanced

In portal and late venous phases, the PHR and septa showed variable CEUS behavior: PHR showed slight hypoenhancement with respect to the adjacent parenchyma in most of the cases (30 out of 38 = 79%) (Figure 3c and 3d) whereas isoenhancement and sustained hyperenhancement occurred in 18.4% and 2.6% of cases, respectively.

The septa showed slight hypoenhancement in 50% of the cases (10 out of 20) (Figure 3c and 3d), whereas in the remaining patients, sustained hyperenhancement and isoenhancement occurred in 35% and 15% of the cases, respectively.

Overall, 4 CEUS PLA patterns could be recognized based on arterial phase findings and reflected evolutive stage of PLA: the initial stage could be considered the type I (the tumor-like pattern), invariably found in small (< 3 cm) PLA due to biliary obstruction (both benign and malignant in origin) when the inflammatory process has caused no or little liquefaction. This pattern represented the most challenging diagnostic dilemma especially when TSE was absent as it occurred in 2 of these 5 cases (Figure 4). TSE and PHR were of high diagnostic values in the other 4 tumor-like PLAs > 3 cm presenting as a prevalently solid hypoechoic area with a small liquified center (Figure 5). CEUS pattern type I accounted for 18.1% of the series. Types II ("honeycomb pattern") (Figure 3b) and III (Figure 6) represent the evolution of PLA due to

the increase in liquified, purulent areas with progressive reduction of septa in number and thickness, until the entire abscessed cavity is occupied by colliquated tissue (type IV) (Figure 7). Types II, III and IV accounted for 27.3%, 18.1% and 36.5% of the cases, respectively.

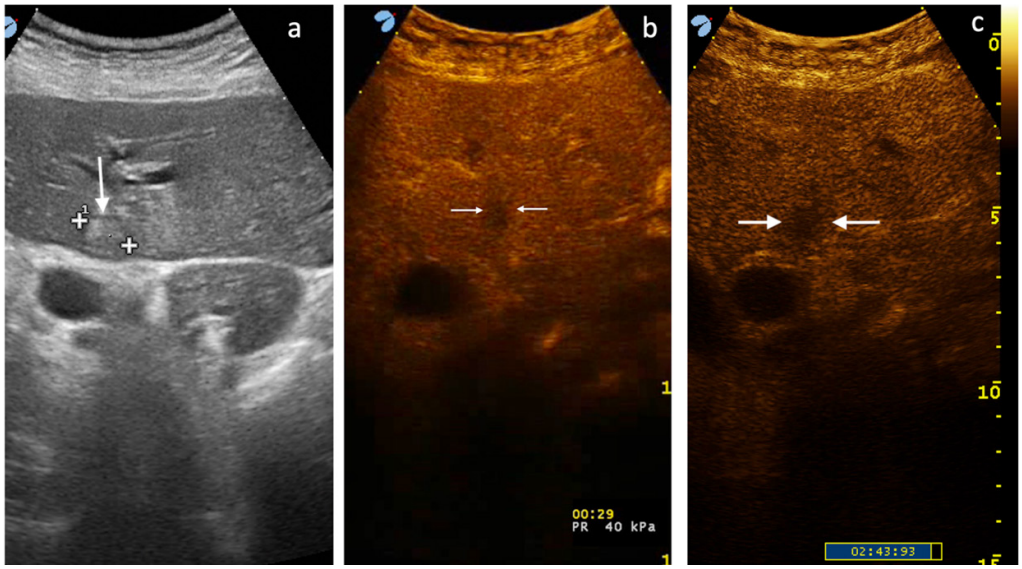

Figure 4. CEUS PLA type I (tumor-like). (a) A 1.6-cm hyperechoic lesion (between markers) with a thin peripheral halo (white arrow) is seen in the left liver lobe; (b) in the arterial phase only an area of hypoenhancement is appreciated (between white arrows), and note that TSE and PHR are not present; (c) in late venous phase wash-out is more evident and the lesion appears more demarcated (between white arrows). Only correlation with clinical and laboratory data made possible the diagnosis of PLA

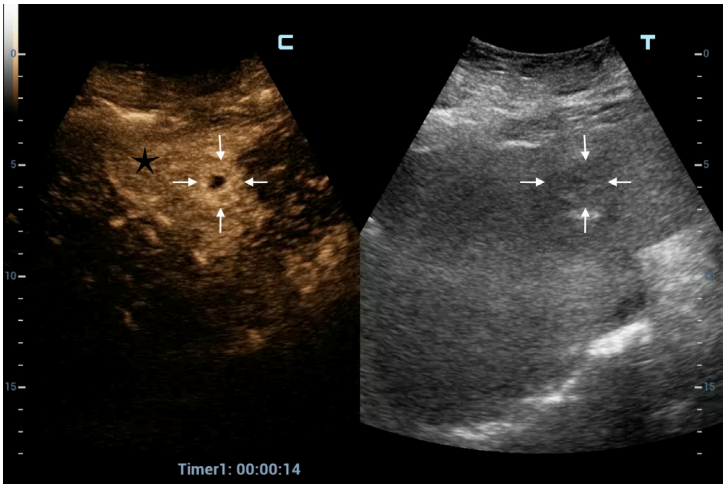

Figure 5. CEUS PLA type I (tumor-like). In this poor visible focal liver lesion (between white arrows in the right split-screen display) all the typical CEUS hallmarks of PLA are present on the left split-screen: TSE (black star); thick PHR (white arrows) and a central non-enhanced area

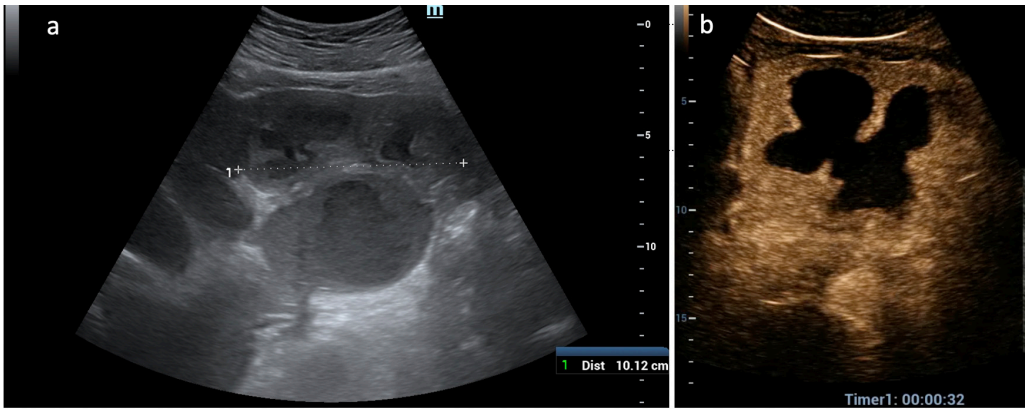

Figure 6. CEUS PLA type III. (a) A complex mass is displayed at US in the left liver lobe; (b) in the arterial phase CEUS demonstrates coalescence of large, liquefied areas with incomplete septa

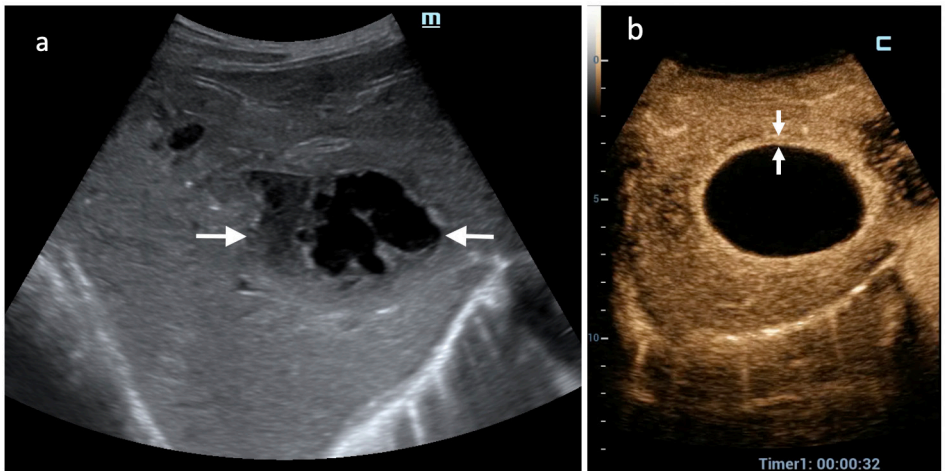

Figure 7. CEUS PLA type IV. (a) A complex mass of the right liver lobe (between white arrows) seems liquified only in part; (b) in the arterial phase the entire mass is non-enhanced, hence totally colliquated. Note the uniform PHR (between white arrows)

There was little correlation between US B-mode and CEUS findings: the only overlapping pattern was the cystic-like (11 cases in B-mode) and (16 cases in CEUS) but in the remaining cases the true internal echostructure of PLA could be elucidated only by CEUS results. Indeed, the presence of internal complete or incomplete septa could not be demonstrated by US B-mode except for in 2 bilobated PLAs.

It is worth mentioning that no patient (even with compromised clinical conditions) had been excluded due to contraindications to the administration of SonoVue. In addition, neither minor nor major adverse events occurred after contrast agent injection in our patients.

Impact on treatment

In 22 cases (67.4%) out of 34 who underwent percutaneous treatment, the operator tailored percutaneous approach according to PLA internal echostructure observed during CEUS exam. Especially in complex masses depicted at conventional US, CEUS better defined the presence of both multiple loculi and communication between them, bringing about the choice of positioning single or multiple catheters (15 cases) (Figure 2). When CEUS showed small liquified areas inside 2 large solid PLAs then NA was deemed sufficient whereas in 5 PLAs with large, not communicating cavities, CD and NA were combined (Figure 8).

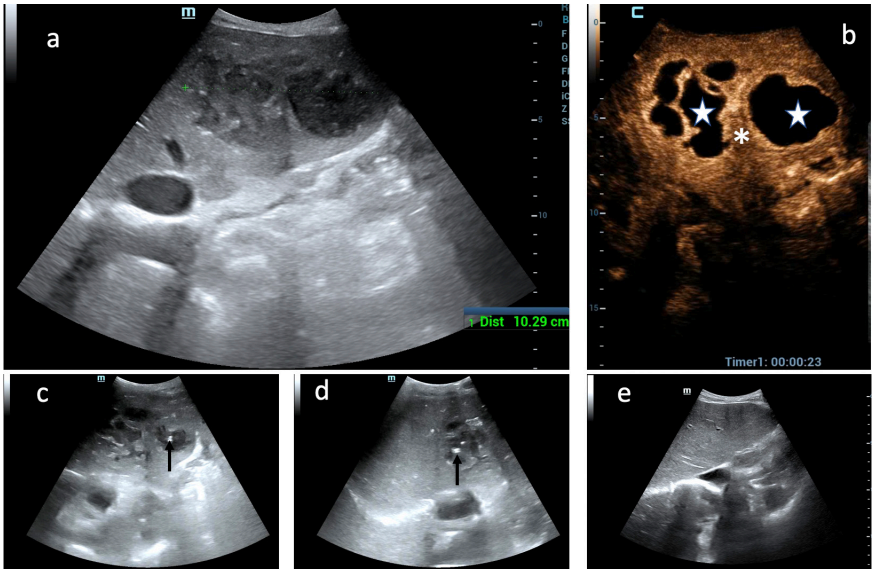

Figure 8. Added value of CEUS to decision-making process for PLA percutaneous treatment. (a) Huge PLA of the left hepatic lobe is displayed as a heterogeneous mass at conventional US; (b) only CEUS definitely shows that two large, not communicating liquified areas (white stars) are separated by a thick septum (white asterisk); (c) the uninoculated medial cavity was aspirated through an 18-g Chiba needle (black arrow point out the needle tip); (d) the multiloculated lateral cavity was drained through a 10-F catheter (black arrow point out the catheter pig-tail); (e) follow-up US scan 4 months after: the left liver lobe in completely healed

In addition, to reach the optimal area for needle puncture not clearly visible on conventional US, CEUS was employed as a guidance system in 4 patients (11.7%).

During follow-up, complete restitutio ad integrum of liver parenchyma was observed in 25 out of 32 patients (73.5%) after percutaneous treatment without relapse; 9 patients did not benefit from interventional procedures due to progression of their underlying neoplastic disease.

Discussion

In this series, a morpho-evolutive classification of PLA based on CEUS findings was built up and CEUS impact on personalized management of patients with PLA was assessed. Although typical CEUS findings (i.e., hyperenhanced rim and non-enhanced cavity in the arterial phase) have been described [15, 16], they mostly refer to fully developed PLA when the entire abscess cavity is filled with necrotic debris and purulent fluid and a thick inflammatory capsule is present. Hyperenhancing internal septa and TSE have been reported as ancillary findings [17–19].

In the present experience, the early arterial phase turned out to be the most diagnostic for PLA since the CEUS hallmarks [TSE, non-enhancing area(s), PHR, hyperenhancing septa] were all appreciated during that phase. Indeed, during the portal and late venous phases, the vascular behavior turned out to be quite variable (a clear wash-out is not often observed for peripheral rim and septa), the only notable exception being TSE which invariably disappeared in portal phase merging with the adjacent parenchyma without true wash-out.

The combination of these signs enabled us to recognize four main CEUS patterns representing different evolutive stages of PLA: from tumor-like aspect (type I) when there is no or little liquified component to mature abscess cavity filled with pus and encircled by an inflammatory capsule (type IV). The latter was the single most frequent pattern (36.5%), the type II ("honeycomb" appearance) ranking second (27.3%). The intermediate stages (type II and III) reflect the progressive liquefaction of the inflamed residual parenchyma inside the abscessed cavity. Recently, Kunze et al. [24] recognized four PLA stages based on correlation between CEUS imaging and pathological findings. Our classification differs for several reasons: 1) multiplicity was considered as an expression of etiology (e.g., in the course of cholangitis) rather than of an evolutive stage; 2) subtypes were avoided to simplify classification: by considering all subtypes, CEUS patterns were as many as 7 in Kunze's classification, with very subtle differences among some of them; 3) the extent and morphology of tissue liquefaction were main criteria of PLA stage identification.

In addition, the role of CEUS in the decision-making process for PLA percutaneous treatment was assessed: in 67.4% of the patients treated by CD and/or NA, CEUS results enabled the operator to choose the most appropriate therapeutic modality by clarifying the internal echostructure of the index PLA. These results support the recent report by Morita et al. [25] that CEUS may be useful for making decisions in the treatment of PLA. These authors concluded that only PLA showing a prevalent solid component (enhanced in the arterial phase) benefited from conservative treatment alone whereas drainage was required when non-enhanced areas were prevalent.

It is worth mentioning that, even if in a minority of patients, CEUS was necessary as guidance modality to reach the largest cavity inside multiloculated PLAs as it occurs in case of percutaneous biopsy or ablation whenever the target is inconspicuous or not visible at US B-mode [26, 27].

In the management of PLA, CEUS offers additional advantages since it does affect the kidney function, and has a high tolerability and safety profile, which can be used in real time without a risk of radiation exposure and hence is repeated to check abscess evolution under treatment.

Moreover, a particular application of CEUS, the so-called intracavitary CEUS (i.e., injection of diluted SonoVue through needle and catheters), allows an interventional clinician to immediately assess needle/catheter placement success, make therapeutic decisions and optimize catheter removal timing [28, 29].

Limitations of this paper should be highlighted: 1) this study is based on a single operator experience whose skills and clinical results may be not reproducible elsewhere; 2) lack of randomization to a control

group (either managed by computed tomography or without CEUS) to verify the added value of CEUS in terms of choice of therapeutic approach; however, it is very difficult if not impossible at all to run such a randomized study in the real life.

In conclusion, CEUS depicts the internal structure of PLA so allowing a morpho-evolutive classification of PLA and provides invaluable information to immediately tailor management to the single case.

Abbreviations

CD: catheter drainage

CECT: contrast-enhanced computed tomography

CEUS: contrast-enhanced ultrasound

NA: needle aspiration

PHR: peripheral hyperenhancing rim

PLA: pyogenic liver abscess

SD: standard deviation

TSE: transient segmental enhancement

US: ultrasound

Declarations

Author contributions

The author contributed solely to the work.

Conflicts of interest

The author declares that he has no conflicts of interest.

Ethical approval

The study was approved by Pineta Grande Hospital Institutional Ethic Committee.

Consent to participate

A written informed consent was obtained from all the patients at the time of admission, with which the tissue, blood and other samples might be used for scientific research but did not relate to patient's privacy.

Consent to publication

Not applicable.

Availability of data and materials

The data analyzed in this study was obtained from Pineta Grande Hospital. Requests for access to these datasets should be directed to archivio@pinetagrande.it.

Funding

Not applicable.

References

1. Bennett JE, Dolin R, Blaser MJ. Mandell, Douglas, and Bennett's principles and practice of infectious diseases. 8th ed. Philadelphia: Elsevier-Saunders; 2015.

2. Chiche L, Dargère S, Le Pennec V, Dufay C, Alkofer B. Abcès à pyogènes du foie. Diagnostic et prise en charge [Pyogenic-liver abscess: diagnosis and management]. Gastroenterol Clin Biol. 2008;32:1077–91. French.
3. Krige JE, Beckingham IJ. ABC of diseases of liver, pancreas, and biliary system. Liver abscesses and hydatid disease. BMJ. 2001;322:537–40.
4. Meddings L, Myers RP, Hubbard J, Shaheen AA, Laupland KB, Dixon E, et al. A population-based study of pyogenic liver abscesses in the United States: incidence, mortality, and temporal trends. Am J Gastroenterol. 2010;105:117–24.
5. Sharma A, Mukewar S, Mara KC, Dierkhising RA, Kamath PS, Cummins N. Epidemiologic factors, clinical presentation, causes, and outcomes of liver abscess: a 35-year Olmsted County study. Mayo Clin Proc Innov Qual Outcomes. 2018;2:16–25.
6. Cerwenka H. Pyogenic liver abscess: differences in etiology and treatment in Southeast Asia and Central Europe. World J Gastroenterol. 2010;16:2458–62.
7. Siu LK, Yeh KM, Lin JC, Fung CP, Chang FY. Klebsiella pneumoniae liver abscess: a new invasive syndrome. Lancet Infect Dis. 2012;12:881–7.
8. Lardière-Deguelte S, Ragot E, Amroun K, Piardi T, Dokmak S, Bruno O, et al. Hepatic abscess: diagnosis and management. J Visc Surg. 2015;152:231–43.
9. Mukthinuthalapati VVPK, Attar BM, Parra-Rodriguez L, Cabrera NL, Araujo T, Gandhi S. Risk factors, management, and outcomes of pyogenic liver abscess in a US safety net hospital. Dig Dis Sci. 2020;65:1529–38.
10. Lai HC, Lin CC, Cheng KS, Kao JT, Chou JW, Peng CY, et al. Increased incidence of gastrointestinal cancers among patients with pyogenic liver abscess: a population-based cohort study. Gastroenterology. 2014;146:129–37.e1.
11. Halvorsen RA, Korobkin M, Foster WL, Silverman PM, Thompson WM. The variable CT appearance of hepatic abscesses. AJR Am J Roentgenol. 1984;142:941–6.
12. Lin AC, Yeh DY, Hsu YH, Wu CC, Chang H, Jang TN, et al. Diagnosis of pyogenic liver abscess by abdominal ultrasonography in the emergency department. Emerg Med J. 2009;26:273–5.
13. Mortelé KJ, Segatto E, Ros PR. The infected liver: radiologic-pathologic correlation. Radiographics. 2004;24:937–55.
14. Benedetti NJ, Desser TS, Jeffrey RB. Imaging of hepatic infections. Ultrasound Q. 2008;24:267–78.
15. Dietrich CF, Nolsøe CP, Barr RG, Berzigotti A, Burns PN, Cantisani V, et al. Guidelines and good clinical practice recommendations for contrast-enhanced ultrasound (CEUS) in the liver-update 2020 WFUMB in cooperation with EFSUMB, AFSUMB, AIUM, and FLAUS. Ultrasound Med Biol. 2020;46:2579–604.
16. Catalano O, Sandomenico F, Raso MM, Siani A. Low mechanical index contrast-enhanced sonographic findings of pyogenic hepatic abscesses. AJR Am J Roentgenol. 2004;182:447–50.
17. Catalano O, Sandomenico F, Nunziata A, Raso MM, Vallone P, Siani A. Transient hepatic echogenicity difference on contrast-enhanced ultrasonography: sonographic sign and pitfall. J Ultrasound Med. 2007;26:337–45.
18. Xie L, Guang Y, Ding H, Cai A, Huang Y. Diagnostic value of contrast-enhanced ultrasound, computed tomography, and magnetic resonance imaging for focal liver lesions: a meta-analysis. Ultrasound Med Biol. 2011;37:854–61.
19. Kishina M, Koda M, Tokunaga S, Miyoshi K, Fujise Y, Kato J, et al. Usefulness of contrast-enhanced ultrasound with Sonazoid for evaluating liver abscess in comparison with conventional B-mode ultrasound. Hepatol Res. 2015;45:337–42.
20. vanSonnenberg E, Wittich GR, Goodacre BW, Casola G, D'Agostino HB. Percutaneous abscess drainage: update. World J Surg. 2001;25:362–9.

21. Trillos-Almanza MC, Restrepo Gutierrez JC. How to manage: liver abscess. Frontline Gastroenterol. 2020;12:225–31.
22. Pang TC, Fung T, Samra J, Hugh TJ, Smith RC. Pyogenic liver abscess: an audit of 10 years' experience. World J Gastroenterol. 2011;17:1622–30.
23. Alkofer B, Dufay C, Parienti JJ, Lepennec V, Dargere S, Chiche L. Are pyogenic liver abscesses still a surgical concern? A Western experience. HPB Surg. 2012;2012:316013.
24. Kunze G, Staritz M, Köhler M. Contrast-enhanced ultrasound in different stages of pyogenic liver abscess. Ultrasound Med Biol. 2015;41:952–9.
25. Morita M, Ogawa C, Omura A, Noda T, Kubo A, Matsunaka T, et al. The efficacy of Sonazoid-enhanced ultrasonography in decision-making for liver abscess treatment. Intern Med. 2020;59:471–7.
26. Francica G, Meloni MF, de Sio I, Terracciano F, Caturelli E, Riccardi L, et al. Biopsy of liver target lesions under contrast-enhanced ultrasound guidance—a multi-center study. Ultraschall Med. 2018;39:448–53.
27. Francica G, Meloni MF, Riccardi L, de Sio I, Terracciano F, Caturelli E, et al. Ablation treatment of primary and secondary liver tumors under contrast-enhanced ultrasound guidance in field practice of interventional ultrasound centers. A multicenter study. Eur J Radiol. 2018;105:96–101.
28. Huang DY, Yusuf GT, Daneshi M, Ramnarine R, Deganello A, Sellars ME, et al. Contrast-enhanced ultrasound (CEUS) in abdominal intervention. Abdom Radiol (NY). 2018;43:960–76.
29. Francica G. Intracavitary contrast-enhanced ultrasound in ultrasound-guided percutaneous management of abdominal fluid collections/abscesses by a single clinician: an example of point-of-care ultrasound. J Ultrasound. 2020;23:175–81.